Characterization of lung cancer by amide proton transfer (APT) imaging: in-vivo study in an orthotopic mouse model

M. Takahashi[1], O. Togao[1], C. W. Kessinger[2], G. Huang[2], I. Dimitrov[1], A. D. Sherry[1], and J. Gao[2]
[1]Advanced Imaging Research Center, UT Southwestern Medical Center, Dallas, Texas, United States, [2]Simmons Comprehensive Cancer Center, UT Southwestern Medical Center, Dallas, Texas, United States

Introduction: Amide proton transfer (APT) imaging is one of the chemical exchange saturation transfer (CEST) imaging methods. With this method the exchange between protons of free tissue water and the amide groups (-NH) of endogenous mobile proteins and peptides is imaged (1). It was demonstrated that APT ratios (APTRs) were found to increase in tumor compared with peritumoral brain parenchyma in an experimental rat glial tumor (2) and human brain tumor (3). In the latter study in patients, the APTRs in 3 low-grade brain tumors were lower than those in 6 high-grade brain tumors, suggesting the ability of APT imaging for characterization of the tumoral grade. The objectives of our study are to test the feasibility of *in-vivo* APT imaging of the lung cancer and to investigate whether the method characterizes the tumoral types. We compared human lung adenocarinoma (A549) and Lewis lung carcinoma (LLC), in an orthotopic mouse model. It is well-known that LLC is a highly malignant cancer and shows more aggressive progression than A549 after transplanted in the lung (4,5).

Materials and Methods: *Animal Preparation:* The orthotopic models of lung cancer in mice were introduced by the method previously reported (4). Briefly, female athymic mice (8-week old, 25-30 g) were injected intravenously via tail vein with 0.5×10^6 A549 cells (n = 6) or 0.5×10^6 LLC cells (n = 6). Tumors were allowed to grow to show approximately $1.0 \times 10^{6\text{-}7}$ relative light intensity on bio-luminescence imaging (BLI) and subjected to the MRI study. All animals were sacrificed and lungs were harvested immediately after the MRI session for histological analysis.
MRI: MRI was conducted with a 7T small animal MR scanner (Varian, Inc, Palo Alto, CA) with a 38 mm birdcage RF coil. Under anesthesia, the mice were tracheaostomized using a non-metallic cannula and connected to a PC-controlled small animal ventilator (flexiVent™, SCIREQ, Quebec, Canada). Each animal was mechanically ventilated at a rate of 33 breaths/min in which the duration of end-expiratory phase was 1.6 s to allow performing the following imaging under respiratory gating. The animals were placed supine with the respiratory sensor, head first with the abdomen centered with respect to the center of a RF coil. After the localizer imaging, axial T2W multi-slice images encompassing the entire lung were obtained with a fast spin-echo sequence (TR/TE = 2500/40 msec; FOV = 30×30 mm; matrix = 128×128; slice thickness = 1 mm; gapless; number of excitations = 8). On a selected 1 mm slab delineating the lung tumor(s), the APT imaging was performed: fast spin-echo images were repeatedly obtained following each presaturation pulse (CW block pulse, B1 = 1.7 μT, duration = 4 s) at 25 saturation points in steps of 0.5 ppm from 6 to -6 ppm. Other parameters were: TR/TE = 5400/8.94 ms, FOV = 30 × 30 mm, ETL = 16, matrix 128 × 64, NEX = 4. A control image without the presaturation pulse was also acquired. Total acquisition time for each animal was approximately 45 minutes. *Image Analysis:* The Z-spectra were fitted through all offsets on a pixel-by-pixel basis according to the procedure using the 12th-order polynomial fitting followed by the correction for B_0 inhomogeneity effect as Salhotra et al. reported (2). MTR asymmetry (MTR_{asym}) was defined as: $MTR_{asym} = S_{sat}(-offset)/S_0 - S_{sat}(+offset)/S_0$, where S_{sat} and S_0 are signal intensities on the images with and without presaturation pulse, respectively. The calculated MTR_{asym} map at the offset of 3.5 ppm is called the APT-weighted image. Circular region-of-interests (ROIs, typical size = 0.34 mm^2) were carefully placed in the tumors. A ROI was also placed in the spinal cord for a reference. *Histopathology:* The tumors were stained with hematoxylin/eosine (HE) for microscopic examination.

Results and Discussion: Figure 1 shows representative T2-weighted images and APT-weighted images of A549 and LLC where the tumors were delineated brighter than the surrounding tissues including spinal cord. The Z-spectrum of LLC (n = 6) was more asymmetric than that of A549 (n = 6), and the S_0/S_{sat} (%) was lower at positive offsets than that at positive offsets (Fig. 2A, B). The MTR_{asym} signal (Fig. 2C) in LLC was consistently higher than that in A549 (at > 1 ppm), with significant differences seen especially at at 2 ppm (6.0 ± 1.8% vs. 2.9 ± 1.5 %, $P = 0.01$) and at 3.5 ppm (3.2 ± 2.9% vs. 0.7 ± 1.3 %, $P < 0.05$). The large APT/CEST effects at 3.5 ppm and 2 ppm in the lung cancer could reflect proton exchange with the backbone amide and side chain amide of the mobile protein/peptide, respectively. The difference in MTR_{asym} between the tumor and spinal cord (Fig. 2D) reached the maximum at 3.5 ppm in both tumors and it was larger in LLC that in A549. The difference between the tumors became maximum at 3-3.5 ppm (7.8 ± 3.9% vs. 2.7 ± 1.9% at 3.5ppm, $P < 0.05$). Histological evaluation revealed higher cell density and larger cell nuclei in LLC compared to A549 (Fig. 3).

We demonstrated the feasibility of the in-vivo APT imaging of the lung cancer in mice. Our data indicates that LLC showed a larger APT effect than A549, which may relate to different protein structures and degree of malignancy. Further studies are under way to investigate the correlation of APT effect with the amount of mobile proton/peptide, or morphology that may cause different background MT effects. APT imaging has the potential to characterize the types of tumor in the lung.

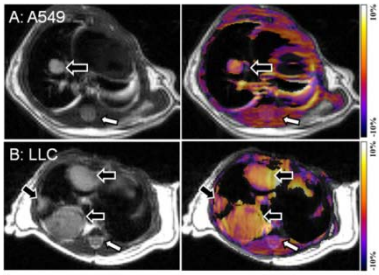

Fig 1. Typical T2-weighted images (left) and APT-weighted images (right) of A549 (**A**) and LLC (**B**).

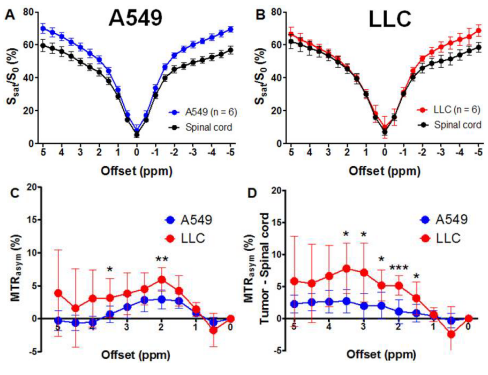

Fig 2. Z-spectra of A549 (**A**) and LLC (**B**) tumors compared to that of spinal cord as a reference. The LLC tumor shows a larger CEST effect than A549 tumor. MTR_{asym} spectra of A549 and LLC (**C**) and difference in MTR_{asym} between the tumor and spinal cord (**D**). LLC shows a larger APT effect than A549 in both analyses, which may relate to the malignancy of the tumors. *, $P \leq 0.05$; **, $P \leq 0.01$; ***, $P \leq 0.001$ by Student's t-test.

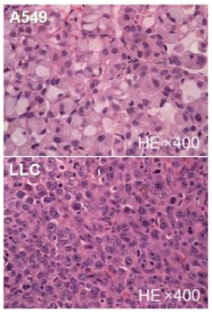

Fig 3. HE staining of A549 and LLC.

Acknowledgment: Authors thank Drs. Zhou and van Zijl at the Johns Hopkins University for data analysis and helpful discussion.

References: 1. Zhou J et al. Nat Med 9:1085-90 (2003). 2. Salhotra A et al. NMR Biomed 21:489-97 (2008). 3. Zhou J et al. Magn Reson Med 60:842-9 (2008). 4. Blanco E et al. Cancer Res 70:3896-904 (2010). 5. Madero-Visbal RA et al. Surg Oncol (2010)